Electronic Supplementary Information

Platinum-palladium-on-reduced graphene oxide as bifunctional electrocatalysts for highly active and stable hydrogen evolution and methanol oxidation reaction

Yingliang Feng,[1] Lihua Zhu,[1,*] An Pei, Sifan Zhang, Kunming Liu,[*] Fengshun Wu, Wenqi Li

Jiangxi Provincial Key Laboratory of Functional Molecular Materials Chemistry, College of Chemistry and Chemical engineering, Faculty of Materials Metallurgy and Chemistry, Jiangxi University of Science and Technology, Ganzhou 341000, Jiang Xi, China

[1] These authors contributed equally to this work.

Corresponding author: zhulihua@jxust. edu.cn (Lihua Zhu); liukunming@jxust.edu.cn (Kunming Liu)

Materials and chemical reagents

Graphene oxide was purchased from Hangzhou Gaonen Technology Co., Ltd. (GO, 10 mg g^{-1}), 2, 2-bipyridine ($C_{10}H_8N_2$, 98%) and ammonium tetrachloropalladate ($(NH_4)_2PdCl_4$) were purchased from Beijing InnoChem Science & Technology Co., Ltd., sodium borohydride ($NaBH_4$) and chloroplatinic acid hexahydrate ($H_2PtCl_6.6H_2O$) were purchased from Shanghai Aladdin Biochemical Technology Co., Ltd, Nafion (5 wt%) was purchased from Shanghai Chulu Industry Co., Ltd., commercial Pt/C (20 wt%) and commercial Pd/C (20 wt%). Absolute methanol (CH_3OH) and absolute ethanol (C_2H_5OH) were purchased from Sinopharm Chemical Reagent Co., Ltd. The chemicals and reagents used are analytically pure without any further purification. Ultrapure water was used in all the experiments. All experiments were performed at room temperature.

Materials characterization

X-ray powder diffraction (XRD) of the samples were analyzed by using a Panalytical X'Pert diffractometer with Cu $K\alpha$ (λ=0.154187 nm) radiation in the scan range of 2θ = 5-90°. X-ray photoelectron spectroscopy (XPS) was applied by the PHI Quantum 2000 (1486.6 eV monochromatic Al $K\alpha$ X-ray source). Transmission electron microscope (TEM), high-resolution transmission electron microscope (HRTEM), scanning transmission electron microscope (STEM) images and STEM-energy dispersive X-ray spectroscopy (STEM-EDS) were obtained by using electron microscope (TECNAI F30) with 300 kV accelerating voltage. Inductively coupled plasma optical emission spectrometry (ICP-OES) was performed by Agilent 730.

Electrochemical testing

HER and MOR electrochemical measurements were used by three-electrode system at the CHI 760E electrochemical workstation (Chenhua, Shanghai, China). All potentials in this work have been corrected to reversible hydrogen electrode (RHE) on the basis of Nernst equation ($E_{RHE} = E_{SCE}$+0.0591 pH+0.2415). The graphite rod was used as the counter electrode in the HER, saturated calomel electrode (SCE) as the reference electrode and carbon paper coated with catalyst ink as the working electrode in 1.0 M KOH solution. 2.0 mg sample was dispersed in a 1.0 mL of mixed solution ($V_{absolute\ ethanol}$: V_{water} = 1:1) and sonicated treatment for 30 minutes. The catalyst ink was evenly dropped onto 1 * 1 cm^{-2} carbon paper, 30 μL 5 wt% nafion was dropped in after the catalyst ink being dried. All HER measurements were performed in N_2-saturated 1.0 M KOH solution. The CV curves were obtained in the non-faradic range of 20-100 mV s^{-1}. The LSV polarization curves were tested at the sweep rate of 5 mV s^{-1} and have been corrected by *iR* compensation. The Nyquist plots were obtained in the frequency range of 0.01-100 kHz.

Pt foil was used as the counter electrode in the MOR, saturated calomel electrode (SCE) as the reference electrode and glass carbon electrode with catalyst ink as the working electrode. 2.0 mg sample was dispersed in a 1.0 mL of mixed solution ($V_{absolute\ ethanol}$: V_{water}= 1:1) and sonicated treatment for 30 minutes. 10 μL catalyst ink was added in two drops to the pre-polished glassy carbon, and being dried, then 5 μL 0.25 wt% Nafion and being dried at room temperature. Firstly, the CV activation step was performed in 1.0 M KOH (N_2-saturation) solution at the potential range of 0.05-1.2 V (vs. RHE). The performance testing was carried out in 1.0 M KOH + 1.0 M CH_3OH solution at the sweep rate of 50 mV s^{-1}. The Nyquist plots were obtained in the frequency range of 0.01-100 kHz in 1.0 M KOH + 1.0 M CH_3OH solution.

The CO-stripping measurements were performed in 1.0 M KOH solution, the solution was purified with N_2 for 30 minutes before testing and then the CV curves were measured within the potential range of 0.05-1.2 V (vs. RHE). In the CO stripping measurement, the CO gas was bubbled into 1.0 M KOH solution at 0.109 V (vs. RHE) for 50 minutes to reach the maximum coverage of the platinum active center CO. Then N_2 was bubbled for 10 minutes at the same voltage to eliminate residual CO in the solution, and the CV curves were also measured at a scan rate of 50 mV s^{-1} over a potential range of 0-1.25 V (vs. RHE).

In overall water splitting testing, both the anode solution and the cathode solution were 1.0 M KOH. In the HER and MOR coupling test, the anode solution was 1.0 M KOH+1.0 M CH_3OH, the cathode solution was 1.0 M KOH, and the anion exchange membrane was used as the membrane.

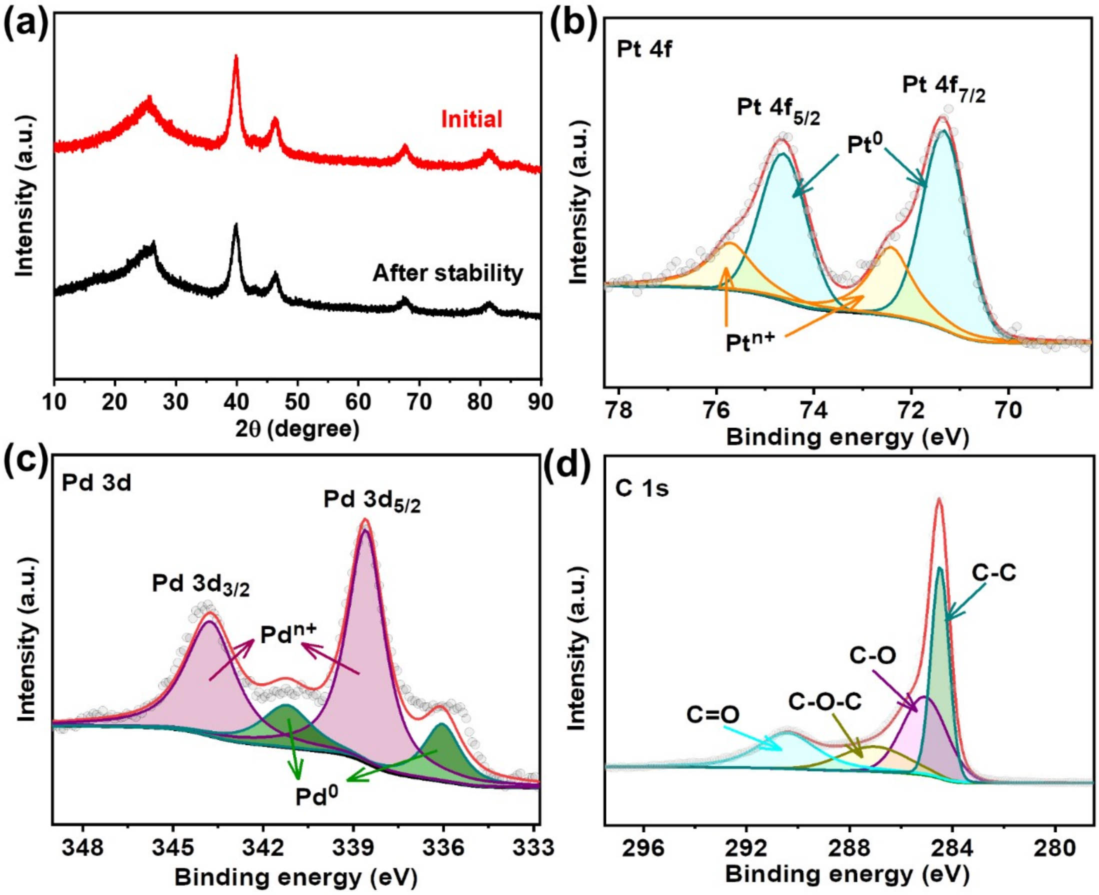

Fig. S1. (a) XRD patterns of PtPd/rGO-2 initial and after stability testing, (b) Pt 4f XPS spectra of PtPd/rGO-2 after stability testing, (c) Pd 3d XPS spectra of PtPd/rGO-2 after stability testing, (d) C 1s XPS spectra of PtPd/rGO-2 after stability testing.

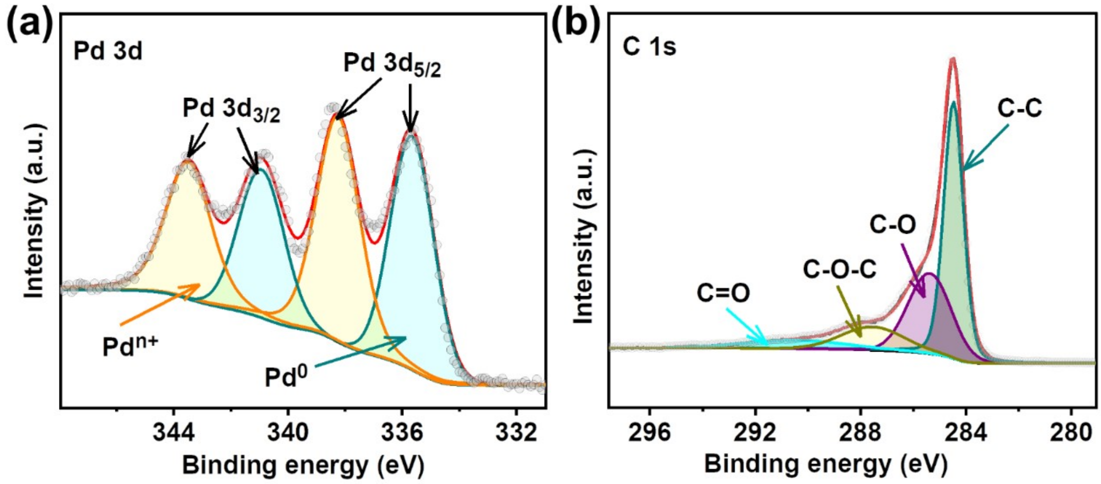

Fig. S2. (a) Pd 3d and (b) C 1s XPS spectra of Pd/rGO.

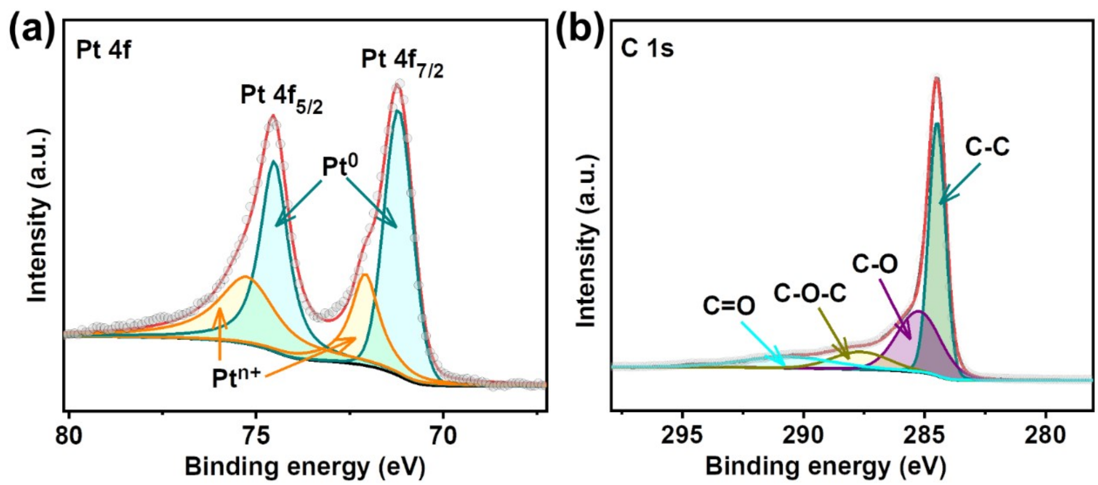

Fig. S3. (a) Pt 4f and (b) C 1s XPS spectra of Pt/rGO.

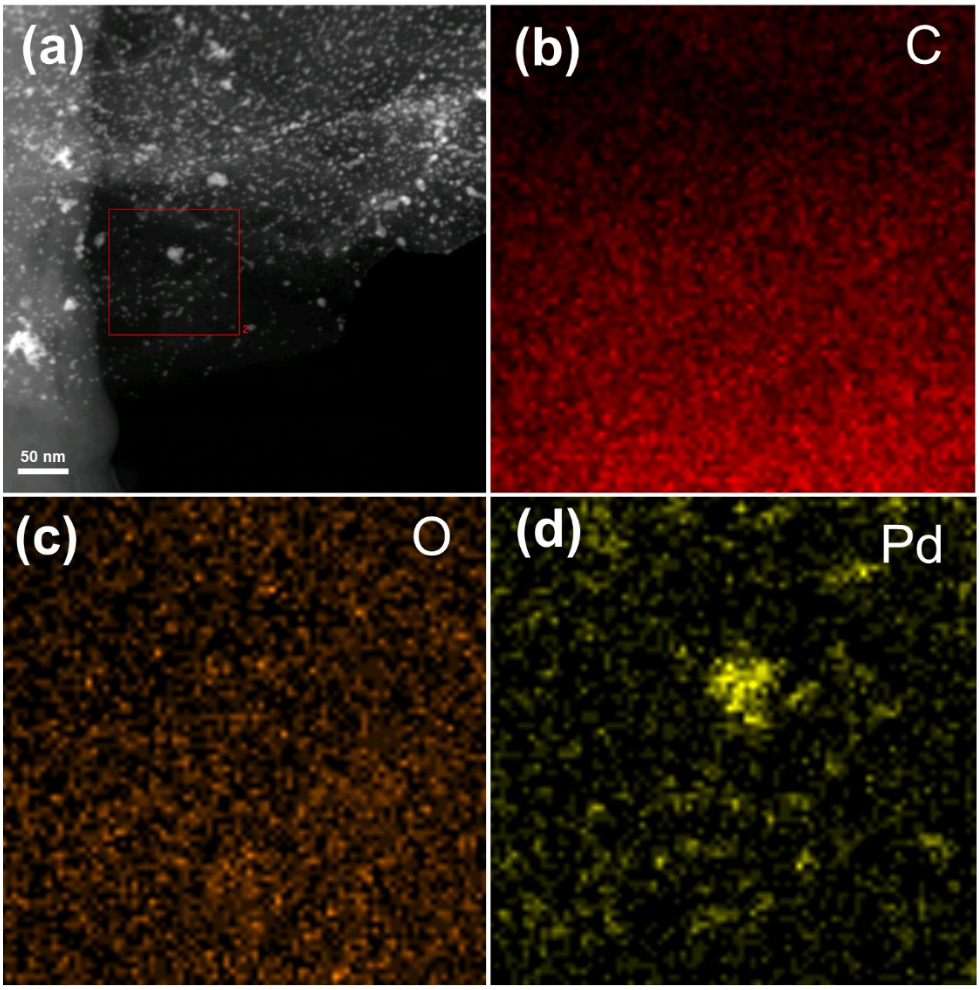

Fig. S4. (a) STEM image of Pd/rGO, STEM-EDS elemental mapping of Pd/rGO (b) C (red), (c) O (orange) and (d) Pd (yellow).

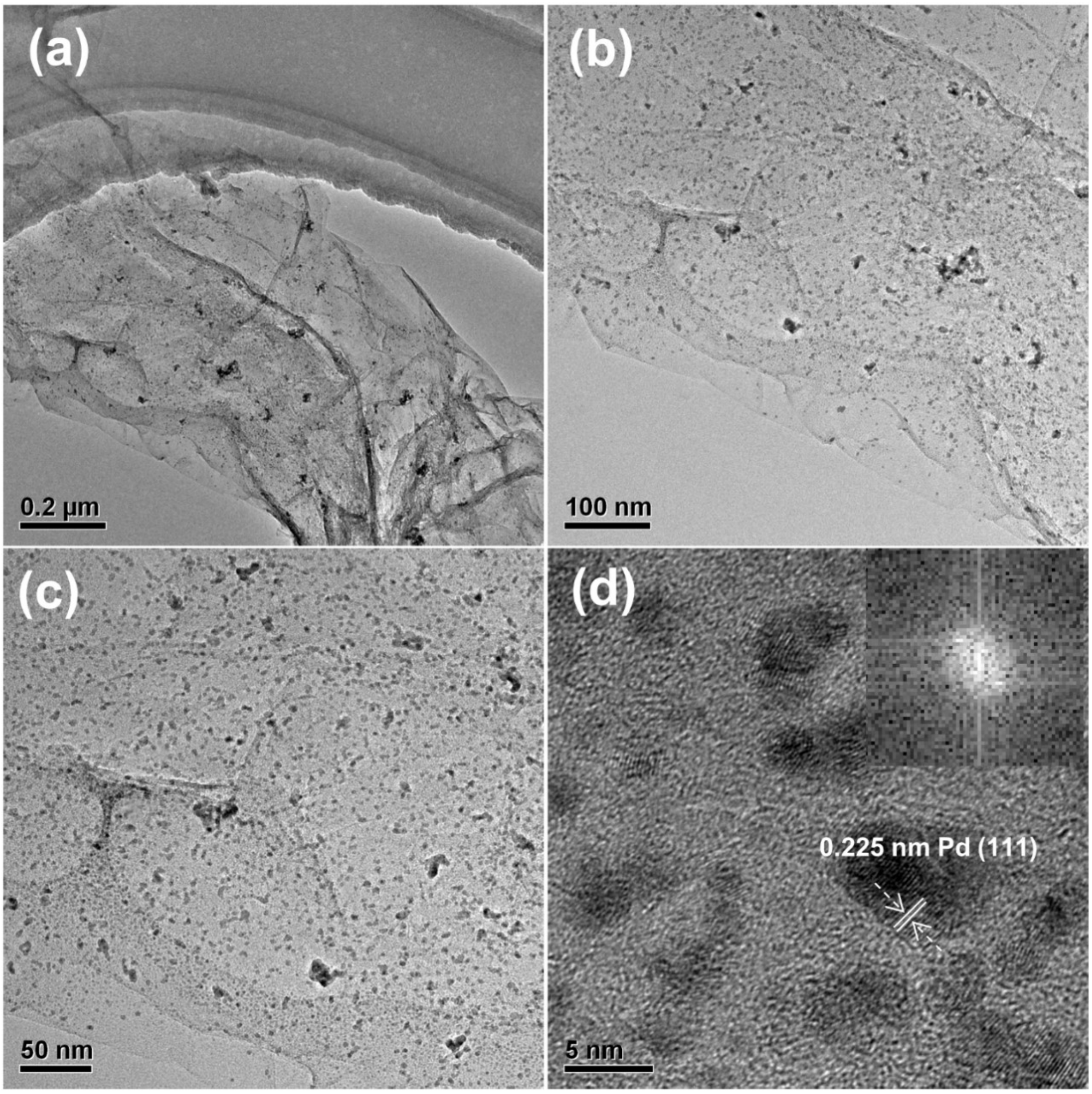

Fig. S5. (a-c) TEM and (d) HRTEM images of Pd/rGO.

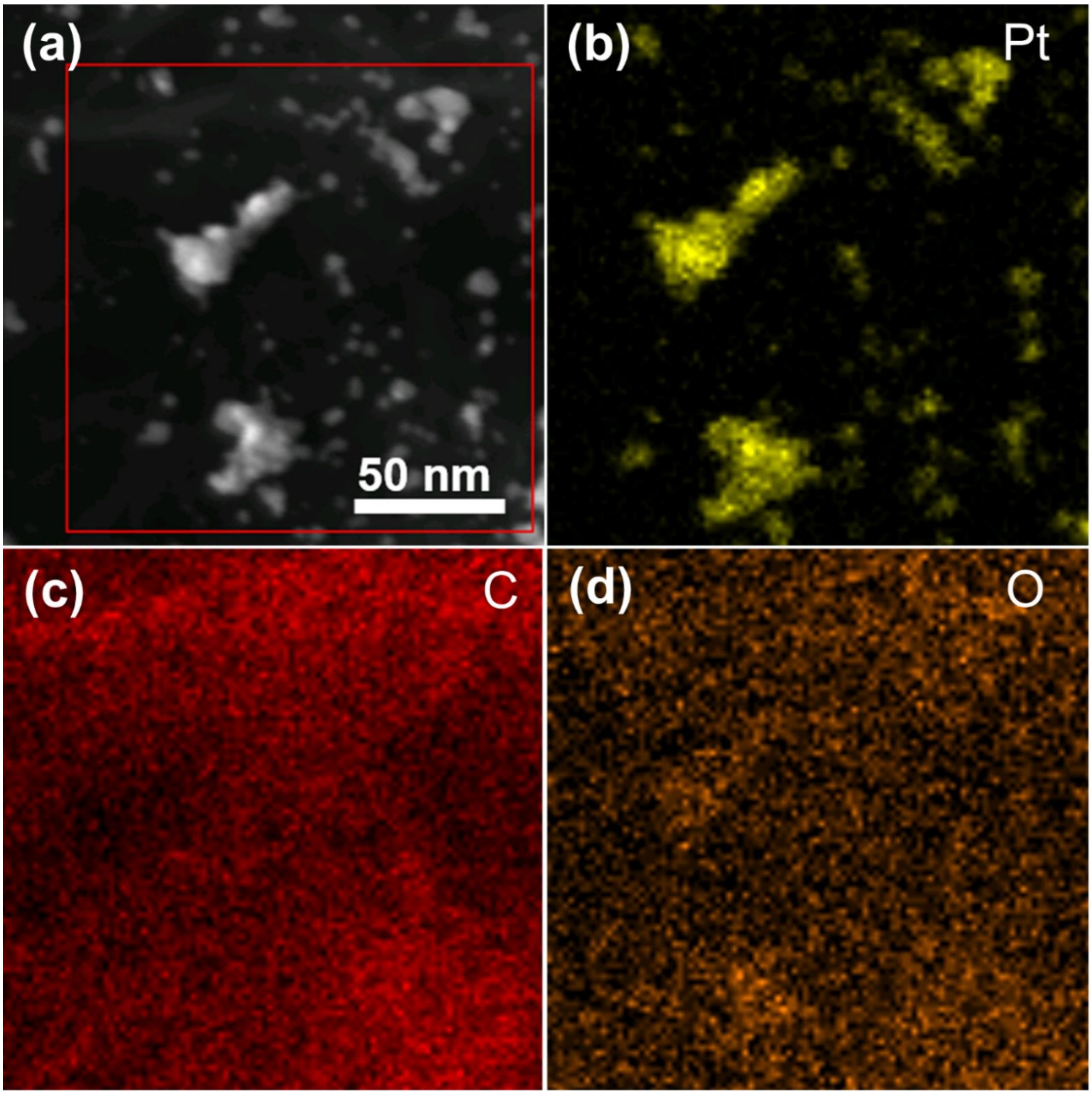

Fig. S6. (a) STEM image of Pt/rGO, STEM-EDS mapping of Pt/rGO (b) Pt (yellow), (c) C (red) and (d) O (orange).

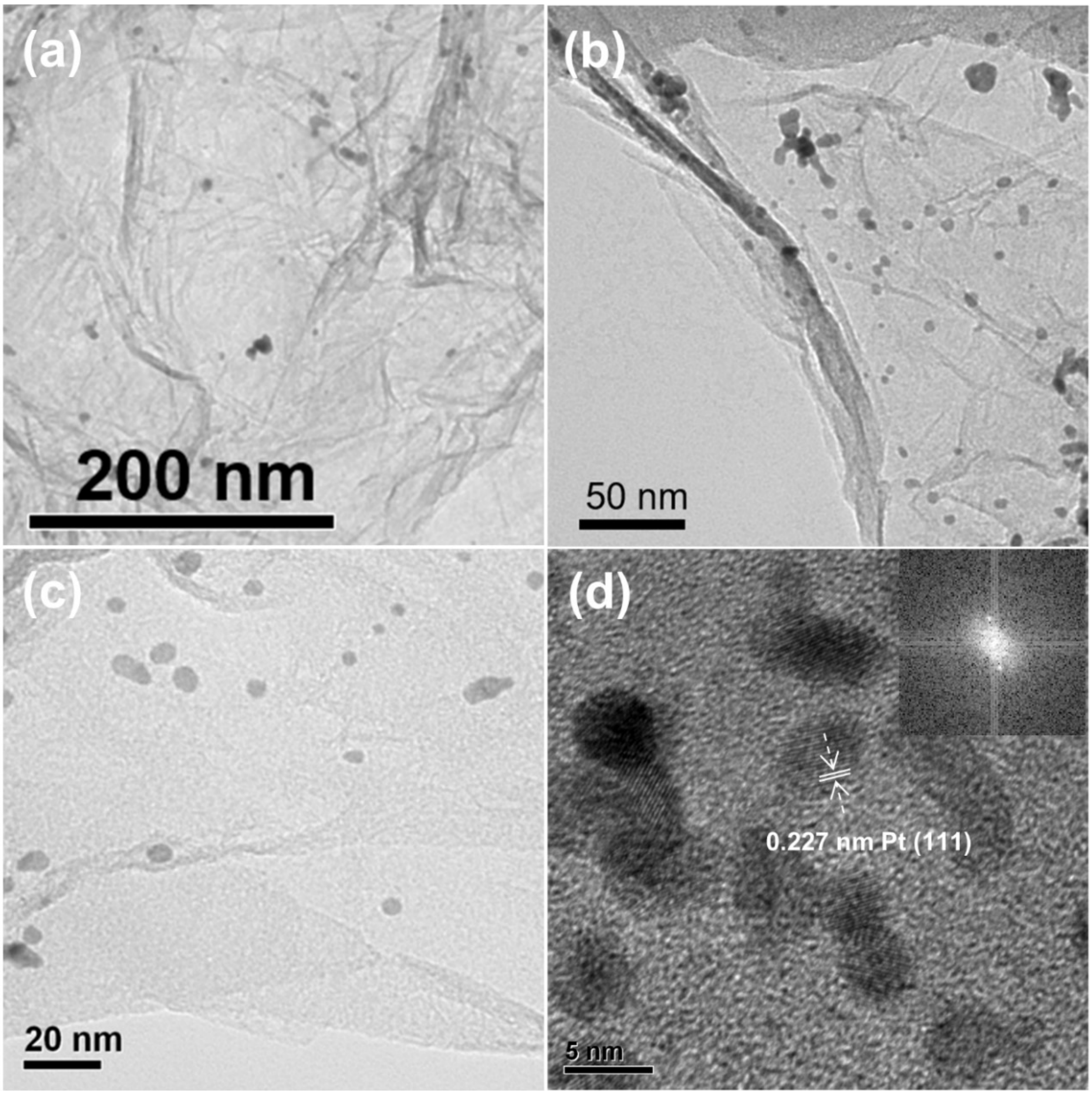

Fig. S7. (a-c) TEM and (d) HRTEM images of Pt/rGO.

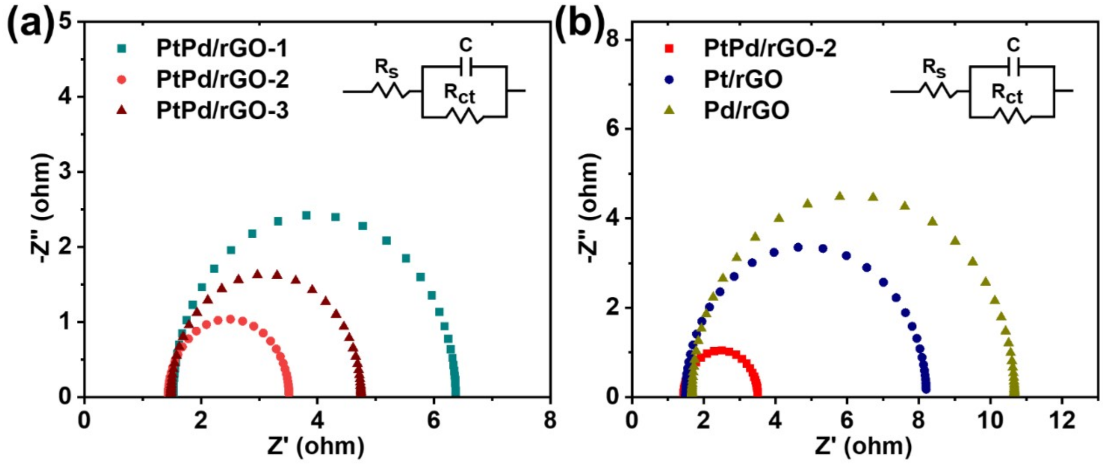

Fig. S8. (a) Nyquist plots of PtPd/rGO-1, PtPd/rGO-2, PtPd/rGO-3, (b) Nyquist plots of PtPd/rGO-2, Pt/rGO, Pd/rGO.

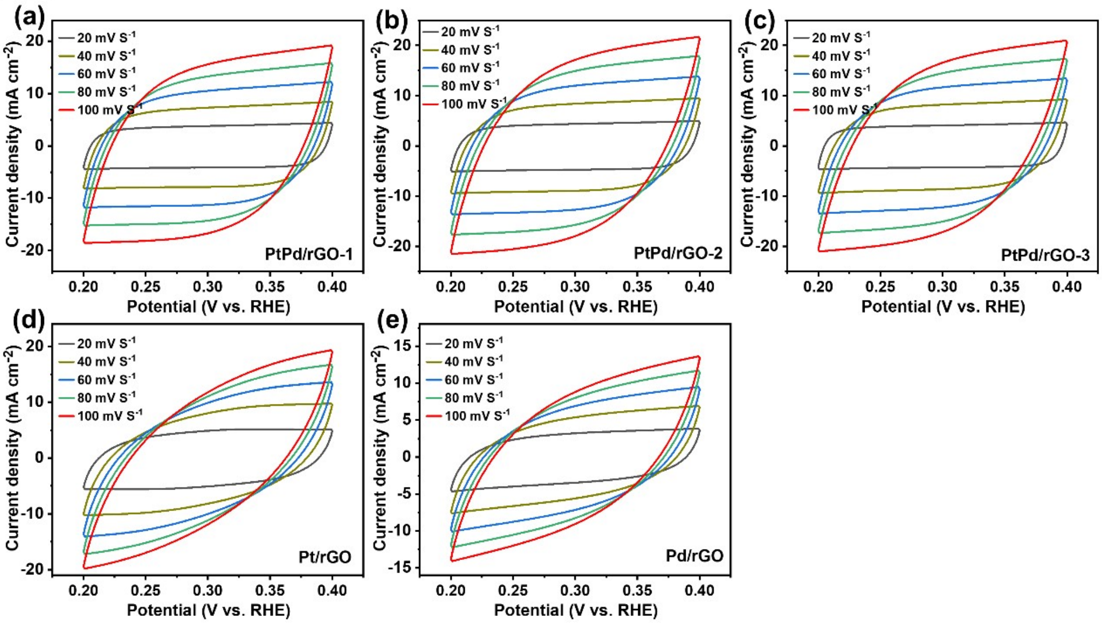

Fig. S9. (a-e) CV curves for the as-synthesized catalysts in the region of 0.2~0.4 V (vs. RHE) with various scanning rates at 20 mV s^{-1}-100 mV s^{-1} for the HER.

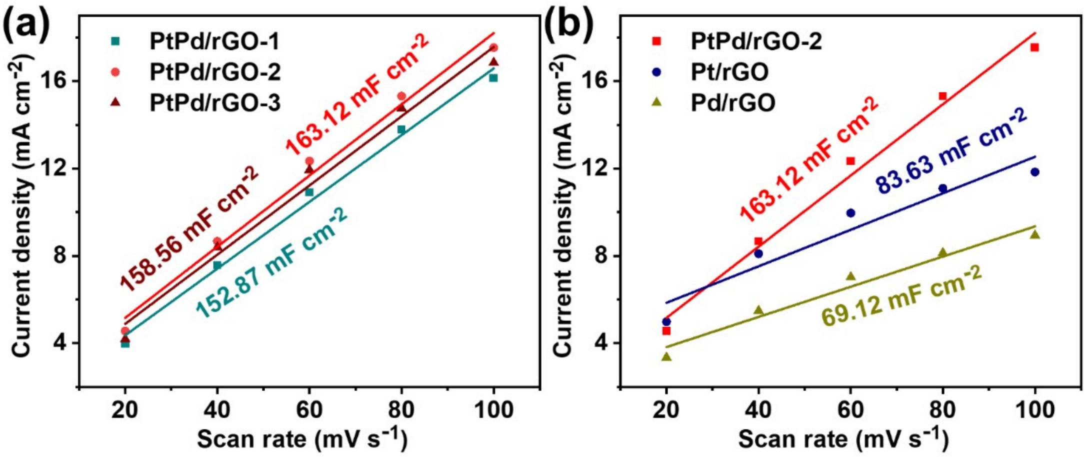

Fig. S10. (a) Cdl of the PtPd/rGO-1, PtPd/rGO-2, PtPd/rGO-3 obtained from CV curves at different scan rates of 20 mV s^{-1}-100 mV s^{-1}. (b) Cdl of the PtPd/rGO-2, Pt/rGO, Pd/rGO obtained from CV curves at different scan rates of 20 mV s^{-1}-100 mV s^{-1}.

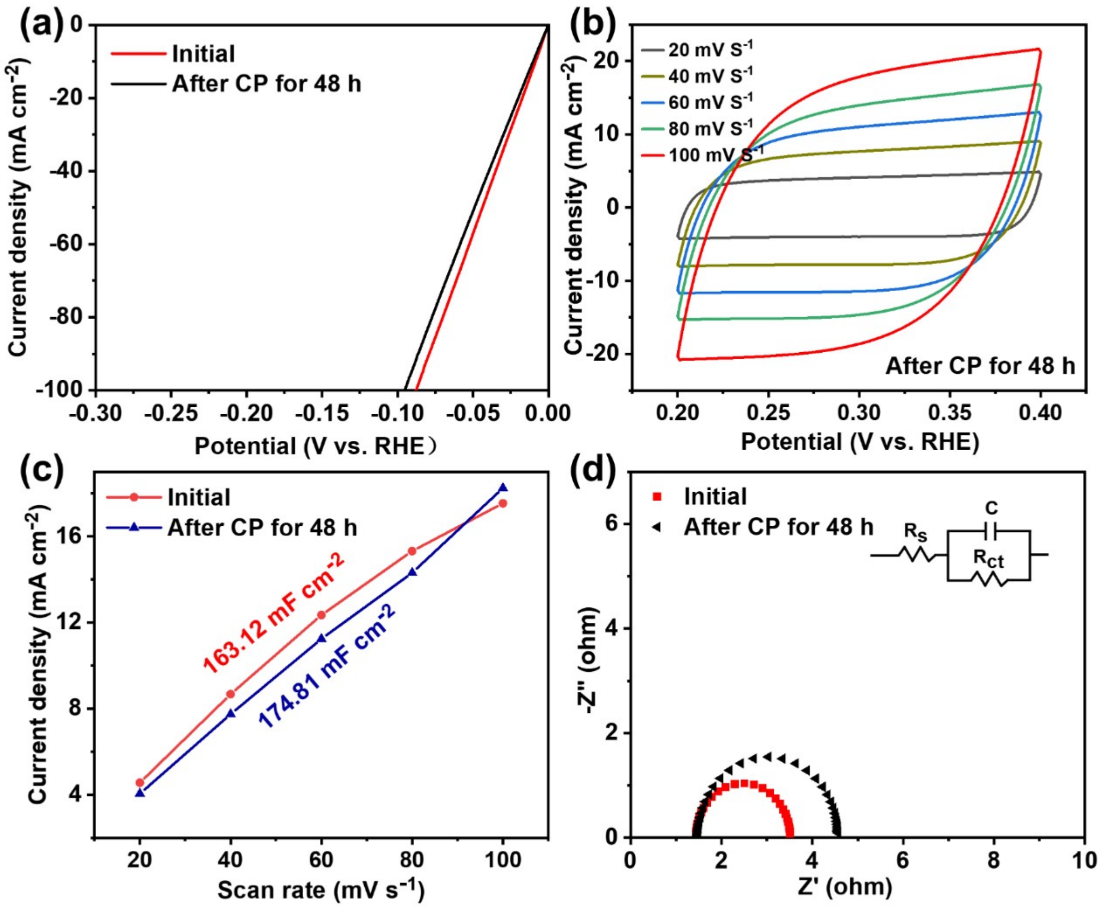

Fig. S11. (a) HER polarization curves of PtPd/rGO-2 initial and after 48 h for chronopotentiometry at 100 mA cm^{-2} in a N_2-saturated 1.0 M KOH solution, (b) CV curves for PtPd/rGO-2 after 48 h for chronopotentiometry at 100 mA cm^{-2} in the region of 0.2~0.4 V (vs. RHE) with various scan rates of 20 mV s^{-1}-100 mV s^{-1} for the HER, (c) Cdl of PtPd/rGO-2 initial and after 48 h of chronopotentiometry at 100 mA cm^{-2} obtained from CV curves at different scanning rates of 20 mV s^{-1}-100 mV s^{-1}, (e) Nyquist plots of PtPd/rGO-2 initial and after 48 h of chronopotentiometry at 100 mA cm^{-2}.

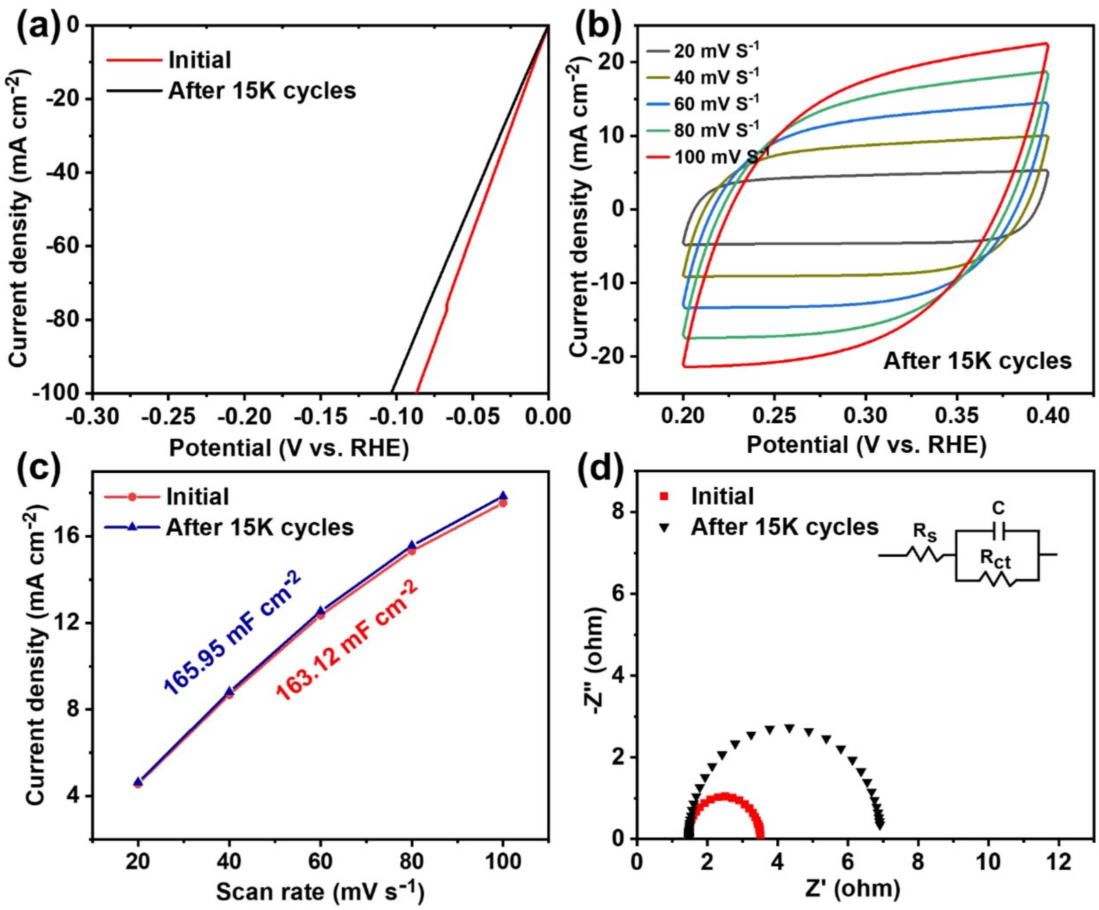

Fig. S12. (a) HER polarization curves of PtPd/rGO-2 initial and after 15000 cycles at 5 mV s^{-1} in a N_2-saturated 1.0 M KOH solution, (b) CV curves for PtPd/rGO-2 in the region of 0.2~0.4 V (vs. RHE) with various scan rates of 20 mV s^{-1}-100 mV s^{-1} for the HER, (c) Cdl of PtPd/rGO-2 initial and after 15000 cycles obtained from CV curves at different scan rates of 20 mV s^{-1}-100 mV s^{-1}, (e) Nyquist plots of PtPd/rGO-2 initial and after 15000 cycles.

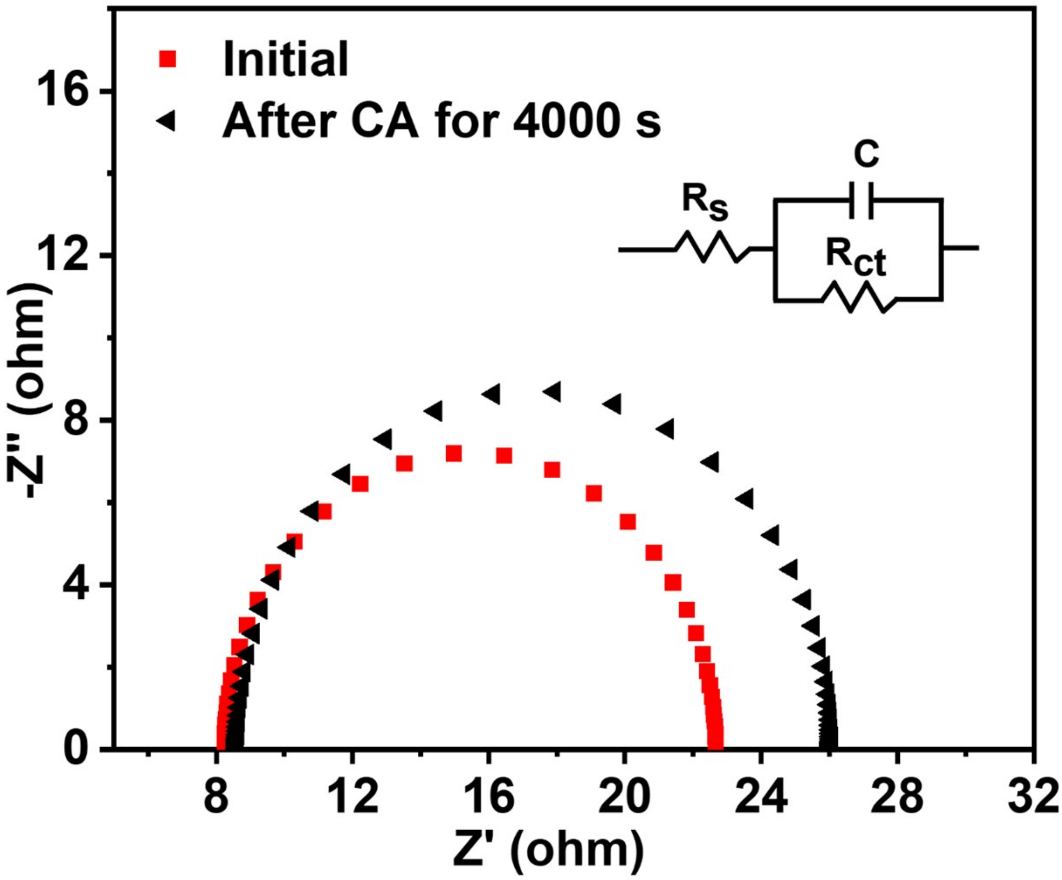

Fig. S13. Nyquist plots of PtPd/rGO-2 initial and after 4000 s chronoamperometry testing in 1.0 M KOH + 1.0 M CH_3OH solution.

Table S1. Comparison of the HER performance of the reported catalysts.

Catalyst	Electrolyte	Overpotential (mV)		Tafel slope
		η_{10}	η_{100}	(mV dec^{-1})
PtPd/rGO-2	1.0 M KOH	9.38	87.16	18.9
Ni@Ni$(OH)_2$/Pd/rGO[1]	1.0 M KOH	76		70
Pt-rGO-300/NiF[2]	1.0 M KOH	34.6		51.58
PtPd@NLS[3]	1.0 M KOH	46		124
SA In-Pt NWs/C[4]	1.0 M KOH	46		32.4
Pt–CoFe@NCNT/CFC[5]	1.0 M KOH	17	93	64.22
Pt@Ni_2–rGO[6]	1.0 M KOH	37		43.0
Pd−Pt-S[7]	1.0 M KOH	71		31
AC Pt-NG/C[8]	1.0 M KOH	35.28		27
Pd-nanodendrites/GNS[9]	1.0 M KOH	39.6		29.7
$Pd_{12}Ru_3$/Ni$(OH)_2$/C[10]	1.0 M KOH	16.1	97	21.8
Ni-HG_1-rGO_1/NF[11]	1.0 M KOH	50	132	48
CS-PdPt[12]	1.0 M KOH	46		88
Pt-PdO/C[13]	1.0 M KOH	29		36

References

1 Z. Deng, J. Wang, Y. Nie and Z. Wei, *J. Power Sources*, 2017, **352**, 26−33.

2 G. Qu, J. Zhou, W. Ji, H. Tang, K. Wei, Y. Zhang, K. Pan and P. Ning, *Chem. Eng. J.*, 2023, **468**, 143764.

3 F. Wen, Y. Zhang, J. Tan, Z. Zhou, M. Zhu, S. Yin and H. Wang, *J. Electroanal. Chem.*, 2018, **822**, 10−16.

4 Y. Zhu, X. Zhu, L. Bu, Q. Shao, Y. Li, Z. Hu, C.-T. Chen, C.-W. Pao, S. Yang and X. Huang, *Adv. Funct. Mater.*, 2020, **30**, 2004310.

5 W. Wang, Z. Jiang, X. Tian, T. Maiyalagan and Z.-J. Jiang, *Carbon*, 2023, **201**, 1068–1080.

6 W. Xu, J. Chang, Y. Cheng, H. Liu, J. Li, Y. Ai, Z. Hu, X. Zhang, Y. Wang, Q. Liang, Y. Yang and H. Sun, *Nano Res.*,2022, **15**, 965–971.

7 J. Fan, K. Qi, L. Zhang, H. Zhang, S. Yu and X. Cui, *ACS Appl. Mater. Interfaces*, 2017, **9**, 18008−18014.

8 M. Sun, J. Ji, M. Hu, M. Weng, Y. Zhang, H. Yu, J. Tang, J. Zheng, Z. Jiang, F. Pan, C. Liang and Z. Lin, *ACS Catal.*, 2019, **9**, 8213−8223.

9 L. Karuppasamy, L. Gurusamy, S. Anandan, C.-H. Liu and J.J. Wu, *Chem. Eng. J.*, 2021, **425**, 131526.

10 A. Pei, G. Li, L. Zhu, Z. Huang, J. Ye, Y.-C. Chang, S.M. Osman, C.-W. Pao, Q. Gao, B.H. Chen and R. Luque. *Adv. Funct. Mater.*, 2022, **32**, 2208587.

11 J. Du, L. Wang, L. Bai, S. Dang, L. Su, X. Qin and G. Shao, *J. Colloid Interf. Sci.*, 2019, **535**, 75–83.

12 B.T. Jebaslinhepzybai, N. prabu and M. Sasidharan. *Int. J. hydrogen energy*, 2020, **45**, 11127–11137.

13 R. Samanta, R. Mishra and S. Barman. *ACS Sustainable Chem. Eng.*, 2022, **10**, 3704–3715.

Table S2. Comparison of MOR performance of the catalysts reported in recent years.

Catalyat	electrolyte	A mg^{-1}
PtPd/rGO-2	1.0 M KOH+1.0 M CH_3OH	10.75
PTSG-2[1]	1.0 M KOH+1.0 M CH_3OH	2.921
PdIn bimetallene[2]	1.0 M KOH+1.0 M CH_3OH	2.27
Au@Pt_1–Pd_1 H-Ss[3]	1.0 M KOH+1.0 M CH_3OH	4.38
SANi-PtNWs[4]	1.0 M KOH+1.0 M CH_3OH	7.93
3D Pt/2D-NiMOF/rGO-4[5]	1.0 M KOH+1.0 M CH_3OH	3.49
PdPtCu MHS@N-G[6]	1.0 M KOH+1.0 M CH_3OH	3.01
Cu@$Pt_{11.3}Pd_{10.1}$[7]	1.0 M KOH+1.0 M CH_3OH	2.387
Pt-Fe_2P/NIR[8]	1.0 M KOH+1.0 M CH_3OH	2.43
IL/Pd_3Cu_1[9]	1.0 M KOH+1.0 M CH_3OH	2.96
Pd-Ir-O/NGS[10]	1.0 M KOH+1.0 M CH_3OH	1.375
Pt_8Ni_2/NH_2-rGO[11]	1.0 M KOH+1.0 M CH_3OH	1.57
Pd-Pd-S[12]	1.0 M KOH+1.0 M CH_3OH	10.2
Pt_1Pd_1-N NFs/CP[13]	1.0 M KOH+1.0 M CH_3OH	9.25

References

1 B. Zhang, F. Yang, X. Ruan, W. Yang, B. Liu and Y. Li, *Ind. Eng. Chem. Res.*, 2020, **59**, 13380−13387.

2 S. Yin, S. Liu, Z. Wang, Y. Xu, X. Li, H. Wang and L. Wang, *Chem. Eng. J.*, 2022, **435**, 134711.

3 W. Liang, Y. Wang, L. Zhao, W. Guo, D. Li, W. Qin, H. Wu, Y. Sun and L. Jiang, *Adv. Mater.*, 2021, **33**, 2100713.

4 M. Li, K. Duanmu, C. Wan, T. Cheng, L. Zhang, S. Dai, W. Chen, Z. Zhao, P. Li, H. Fei, Y. Zhu, R. Yu, J. Luo, K. Zang, Z. Lin, M. Ding, J. Huang, H. Sun, J. Guo, X. Pan, W.A. Goddard III, P. Sautet, Y. Huang and X. Duan, *Nat. Catal.*, 2019, **2**, 495–503.

5 J. Qiu, Y. Han, K. Zhang, Y. Deng, Y. Wu and L. Yan, *ACS Appl. Energy Mater.*, 2022, **5**, 4439−4447.

6 L. Sun, H. Lv, D. Xu and B. Liu, *J. Mater. Chem. A*, 2020, **8**, 15706–15714.

7 S. Zhou, R. Yan and W. Zhou, *Adv. Mater. Interfaces*, 2022, **9**, 2200761.

8 Z. Xu, J. Hu, H. Dong, Y. Zhu and M. Zhu, *J. Colloid Interf. Sci.*, 2022, **626**, 599–607.

9 H. Wang, S. Zhang, W. Cai, B.Z. Xu, Z. Cai, Y. Wu, X. Luo, X. Wei, Z. Liu, W. Gu, A. Eychmüller, C. Zhu and J. Chen, *Mater. Horiz.*, 2020, **7**, 2407–2413.

10 J. Shu, R. Li, Z. Lian, W. Zhang, R. Jin, H. Yang and S. Li, *J. Colloid Interf. Sci.*, 2022, **605**, 44–53.

11 Y. Chen, Y. Ma, Y. Zhou, Y. Huang, S. Li, Y. Chen, R. Wang, J. Tang, P. Wu, X. Zhao, C. Chen, Z. Zhu, S. Chen, K. Cheng and D. Lin, *Int. J. hydrogen energy*, 2022, **47**, 6638–6649.

12 J. Fan, K. Qi, L. Zhang, H. Zhang, S. Yu and X. Cui, *ACS Appl. Mater. Interfaces*, 2017, **9**, 18008−18014.

13 Y. Zhang, G. Shu, Z. Shang, K. Ma, L. Song, C. Wang, C.-A. Zhou and H. Yue, *ACS Sustainable Chem. Eng.*, 2023, **11**, 8958–8967.